Title

Centrifuge modelling of energy foundations in sand

ISBN

9781138022225

Authors

Goode, J
Zhang, M
McCartney, J

Publication Date

2014-01-06

DOI

10.1201/b16200-100

Peer reviewed

Centrifuge modelling of energy foundations in sand

J.C. Goode, III, M. Zhang, and J.S. McCartney
University of Colorado Boulder, Boulder, USA

ABSTRACT: This paper presents the results from a series of centrifuge tests to understand the strain distribution in semi-floating energy foundations in dry Nevada sand during mechanical loading and foundation heating. In addition to the details of the model reinforced-concrete energy foundation, the results from 1-g thermo-mechanical characterization tests are presented. The centrifuge-scale tests involve application of an axial load to the head of the foundation (in load-control conditions) then circulation of a heat exchange fluid through embedded tubing to bring the foundation to a constant temperature. During this time, the axial strains are measured using embedded strain gages, and the soil and foundation temperatures and thermal and thermo-mechanical head displacements are monitored. Loading tests to failure were then performed on the foundations to characterize the impact of temperature on the load-settlement curve. The information from the tests permits definition of soil-structure interaction parameters for dry sands under realistic stress states. Different from previous studies on unsaturated silt, no change in ultimate side shear resistance was observed with increasing temperature. The thermal strains are relatively constant with depth and are close to free expansion.

1 INTRODUCTION

Although incorporation of heat exchangers into deep foundation elements (energy foundations) helps reduce the installation costs of ground-source heat exchange systems (Brandl 1998; Ennigkeit and Katzenbach 2001; Brandl 2006), an issue encountered is the potential for foundation movements due to thermal expansion and contraction of the foundation or surrounding soil. Further, soil-structure interaction may restrain movement of the foundation, leading to generation of thermally induced stresses. This behavior has been documented in several field-scale case histories (Laloui et al. 2006; Bourne-Webb et al. 2009; Amatya et al. 2012; McCartney and Murphy 2012). Although thermo-mechanical soil-structure interaction analyses permit prediction of changes in axial stress or strain during heating and cooling operations (Knellwolf et al. 2011; Plaseied 2011), they require empirical data for calibration of model parameters and verification of predictions.

Centrifuge modeling is a useful approach to measure empirical parameters for soil-structure interaction analyses for energy foundations, as the properties of scale-model foundations and soil layers can be carefully controlled and different configurations can be considered for lower costs than full-scale field testing. An additional benefit of centrifuge modeling is that scale-model energy foundations can be loaded to failure to characterize the effects of temperature on the load-settlement curve. The back-calculated ultimate side shear stress distribution and end bearing are useful parameters for soil-structure interaction analyses. Further, centrifuge tests on scale-model foundations with embedded instrumentation permit measurement of thermally induced stresses and strains in the foundation, which can be used to validate soil-structure interaction analyses or finite element models.

The objective of this study is to quantify axial strain distributions in semi-floating energy foundations within a dry sand layer during foundation heating under free head expansion conditions and subsequent mechanical loading to failure. This study builds upon centrifuge programs at the University of Colorado Boulder. McCartney and Rosenberg (2011) performed non-isothermal loading tests on semi-floating energy foundations in compacted silt to quantify the impact of temperature on the ultimate capacity of energy foundations. An increase in side shear resistance with temperature was attributed to the differential expansion of the foundation and surrounding soil as well as thermally induced water flow in the unsaturated silt. Stewart (2012) used embedded strain gages in energy foundations to evaluate the impact of end boundary conditions on the thermal axial strains in compacted silt.

2 BACKGROUND

2.1 *Stress-Strain Response of Energy Foundations*

As an energy foundation is heated or cooled, it may expand or contract, depending on the constraint conditions. For unconstrained conditions, the axial thermal strain can be calculated as follows:

$$\varepsilon_{T,free} = \alpha_c \Delta T \quad (1)$$

where α_c is the coefficient of linear thermal expansion of reinforced concrete, and ΔT is the change in temperature. Thermal strain is defined as positive for compression. Accordingly, α_c is negative as structural elements expand during heating (positive ΔT). The value of $\varepsilon_{T,free}$ is an upper limit on the thermal strains due to heating or cooling. For constrained conditions, the actual thermal strains will be less than those predicted by Eq. 1. In this case, the thermal axial stresses induced in an energy foundation can be calculated as follows:

$$\sigma_T = E\left(\varepsilon_T - \alpha_c \Delta T\right) \quad (2)$$

where E is the Young's modulus of reinforced concrete and ε_T is the axial thermal strain. For energy foundations embedded in soil or rock, soil-structure interaction mechanisms will restrict the movement of the foundation during heating. Specifically, the side shear resistance, end bearing, and stiffness restraint of the overlying building will lead to different distributions in thermally induced stresses and strains in an energy foundation (Laloui et al. 2006; Bourne-Webb et al. 2009; Amatya et al. 2012; McCartney and Murphy 2012).

2.2 *Centrifuge Modeling of Energy Foundations*

Centrifuge modeling relies on the concept of geometric similitude, which assumes that a full-scale prototype soil layer will have the same stress state as a model-scale soil layer that is N times smaller when spinning in a geotechnical centrifuge at a centripetal acceleration that is N times larger than that of earth's gravity (Ko 1988; Taylor 1995). Geometric similitude can be employed to extrapolate the load-settlement behavior and thermal soil-structure interaction phenomena of scale-model energy foundations to those of full-scale prototype foundations. Lengths scale by a factor of 1:N (model:prototype), strains scale by a factor of 1:1, and forces scale by a factor of $1:N^2$. An issue in modeling energy foundations is that the temperature does not depend on the increased body forces in the centrifuge. Spatial measurements of temperature in dry quartz sand surrounding a cylindrical heat source during centrifugation at different g-levels by Krishnaiah and Singh (2004) confirm that centrifugation does not lead to a change in the heat flow process. However, if the dimensions associated with the spatial distribution of heat flow were scaled from model to prototype scale (assuming the same thermal conductivity in both cases), the time required for heat flow by conduction would be N^2 times faster in the centrifuge model ($1:N^2$). Saviddou (1988) derived this scaling factor from the diffusion equation, which only includes scaling of the length. An implication of scaling is that a greater volume of soil surrounding the foundation in prototype scale will be affected by changes in temperature. Soils change in volume with temperature, so if a greater zone of soil around the foundation is affected then the effects of differential volume change of the foundation and soil may be emphasized. From this perspective, scaling may provide a worst-case scenario. If the goal of testing is to evaluate the impact of temperature on the axial strain distribution in the foundation, tests can be performed until strains stabilize for a given temperature. Alternatively, numerical simulations can use model scale data instead of prototype scale data.

3 MATERIALS

3.1 *Scale-Model Foundations*

A scale-model energy foundation was fabricated to study the impact of mechanical loading and heating on the internal strain distribution in energy foundations. The foundation has a diameter of 63.5 mm, and a length of 342.9 mm. A centrifuge acceleration of 24g was used throughout this study, so the corresponding prototype-scale foundation lengths 8.2 m with a diameter of 1.5 m. The foundation is tested in a soil layer having a thickness of 533.4 mm. Although drilled shafts are typically cast-in-place, the model foundation was precast in a cardboard mold to ensure quality construction considering the extensive instrumentation. This approach also allows for characterization of the mechanical and thermal properties of the foundation. The foundation has a larger diameter than that of Stewart (2012) to provide more space around embedded instrumentation. Further, the larger diameter permitted a larger fraction and size of coarse aggregates to be incorporated into the concrete mix design. This led to a Young's modulus of reinforced concrete that was closer to that of drilled shaft foundations in the field than obtained by Stewart (2012).

The reinforcing cage was formed from welded steel hardware cloth that simulates the longitudinal and lateral members of a steel reinforcing cage. The cage has 12.7 mm square openings, with 19 gage wire thickness. The cage diameter is 48.5 mm with 7.5 mm of concrete cover on the sides. The cage has 6.35 mm of concrete cover on the top and bottom. A schematic of the foundation is shown in Figure 1.

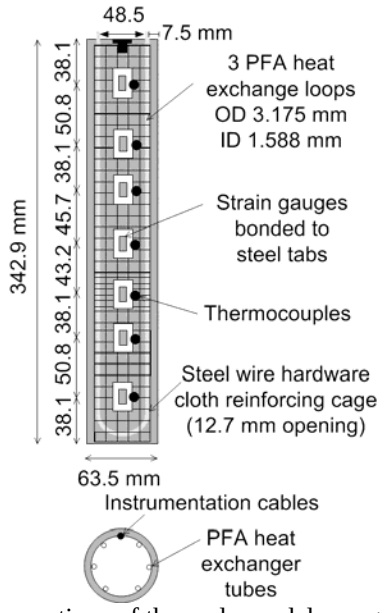

Figure 1. Cross-sections of the scale-model energy foundation.

Seven strain gages and thermocouples were embedded within the foundation to characterize the strain response and temperature distribution within the foundation. The strain gages were model CEA-13-250UW-350 from Vishay Precision Group, and were bonded using M-Bond AE-15 epoxy to 50.8 mm-long, 12.7 mm-wide, and 1.8 mm-thick steel tabs. The tabs have two 6.1 mm-diameter holes at top and bottom for good interaction with the concrete. The zinc plating on the steel was sanded off to provide a smooth steel surface. The epoxy was used as the bonding agent due to its ability to withstand cyclic temperatures. The bonded gages were cured under pressure for 4 hours at 57.2 °C. A Teflon strip was placed over the cured gage, which was then covered using a waterproof epoxy (Gagekote #5). Miniature thermocouples (Fine wire type K Model STC TT K 36 3C from Omega) were attached to the steel tabs next to the strain gages. Thermo-mechanical calibration tests were performed on the individual gages by hanging a 27 kg weight from the steel tabs, then heating the gage with a hot air gun. The results of one of the calibration tests on a gage-tab assembly are shown in Figure 2.

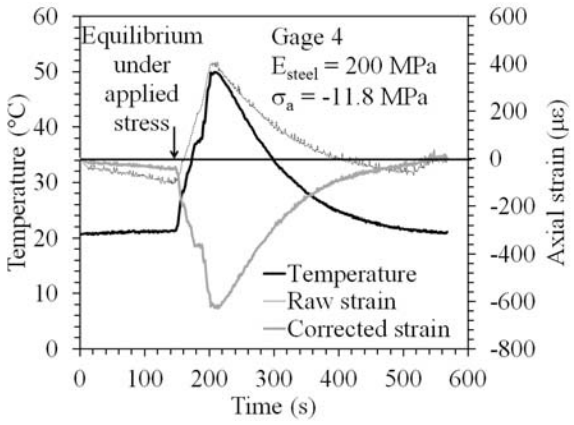

Figure 2. Correction of a strain gage attached to a steel tab.

After reversing the sign of the gage reading so that compression is defined as positive, the raw gage reading shows negative strains during application of the tensile force. However, heating was observed to lead to a reversal of the trend in strain. This unexpected behavior occurs due to differential thermal expansion of the gage, steel tab, and the epoxy. To account for this behavior, a thermo-mechanical correction was applied so that the gages would yield a Young's modulus of E_{steel} = 200 GPa and a coefficient of linear thermal expansion of α_{steel} = -13.0 με/°C, as follows:

$$\varepsilon_{corrected} = \chi \varepsilon_{measured} + \Delta T \beta \quad (3)$$

where χ and β are mechanical and thermal correction factors defined for each gage. The values of χ ranged from 0.34 to 0.52 and the values of β ranged from -24.9 to -28.4. These values differed due to variations in the construction of the gages.

The finished strain gages were then attached to the inside of the reinforcing cage using thin wire thread. The placement of the gages is shown in Figure 1. Three heat exchanger loops were affixed to the reinforcement cage. The loops were equally spaced around the circumference of the cage and affixed to the cage with small cable stays. Perfluoroalkoxy (PFA) tubing with an inside diameter of 3.175 mm was used for the heat exchange loops, with the bottom loops held tight to the cage in order to avoid loops crossing the bottom of the cage.

A cardboard tube with a 63.5 mm inside diameter was used as the form for the concrete. The cage was centered in the form, and concrete having a 1:2:1.5:1.5 water:cement:sand:coarse aggregate mixture was poured into the form using a miniature tremie pipe to ensure uniform concrete placement. Concrete placement was performed on a large vibrating table to guarantee the concrete was flowing to all areas of the form as well as extruding entrapped air. When the concrete had reached the top of the form, a hex-head bolt was placed in the middle of the foundation to provide a centering point for mechanical loading of the foundation. The foundations were cured in a fog room for 14 days, after which 14 more days of curing were permitted after removing the form.

Axial stresses were applied to the foundation in 1g in 70 kPa increments up to 350 kPa to evaluate the elastic properties of the reinforced concrete. A linearly variable differential transformer (LVDT) was used to measure the head displacement of the foundation. Although the strains varied slightly with height, due potentially to off-axis loading, the average corrected strains indicate that the reinforced concrete has a Young's modulus of about 33 GPa.

A free-expansion heating test was performed on the foundation by circulating water having a temperature of 55 °C through the heat exchange tubing. The axial strains were measured using the embedded strain gages and the head displacement was measured using the LVDT. The global strain inferred from the LVDT displacements (approximately 0.11 mm expansion of the 342.9 mm-long foundation during a change in temperature of 21 °C) indicates that the reinforced concrete has a coefficient of thermal expansion of a_c of -16 με/°C. During the free expansion test, it was expected that all of the gages would show the same strain value. Although the strain values corrected using Equation 3 give mobilized coefficients of thermal expansion close to the global expansion of the foundation, they were consistent. This was attributed to the differential expansion of the steel tabs and the surrounding concrete, slight variations in the alignment of the gages, and variations in the steel-concrete interaction. Accordingly, an additional calibration term $\Delta T\xi$ was added to Eq. 3, with values of ξ ranging from 3.8 to 10 defined so that the gages shows the same slope as the global thermal expansion strain defined from the LVDT displacements. Gages 2 and 6 did not function reliably and are not included in the analysis.

3.2 *Soil*

The soil used in this study is dry Nevada sand having a relative density of 60% (void ratio of 0.75). This soil was selected as its shear strength is expected to increase with depth, in contrast to the behavior of the unsaturated silt used by Stewart (2012), which had uniform shear strength with depth. The sand consists of uniform angular particles, with characteristic grain size values of D_{10} = 0.09 mm, D_{30} = 0.11 mm, and D_{60} = 0.16 mm. The sand has a friction angle of 35°, a shear modulus of 30 MPa, and a Poisson's ratio of 0.3 at this relative density and a mean stress 100 kPa. The thermal conductivity measured using a KD2Pro thermal needle was found to be 0.25 W/mK.

4 EXPERIMENTAL SETUP

4.1 *Container and Instrumentation*

A schematic of the container used for testing of the foundations is shown in Figure 3. The container is an aluminum cylinder with an inside diameter of 0.6 m, wall thickness of 13 mm, and a height of 0.54 m. A 13 mm-thick insulation sheet was wrapped around the container to prevent heat transfer through the sides of the cylinder (no-flow boundary). The uninsulated bottom of the container permits some loss of heat, but this was preferred to have a stiff platform for loading. Loads were applied to the foundation using a pneumatic Bellofram piston, and were measured using a load cell.

The locations of instrumentation incorporated into the centrifuge container are shown in Figure 3. Two LVDTs attached to beams spanning between two support beams were used to monitor movement of the foundation head and deflections of the soil surface. Thermocouple profile probes were inserted into the sand at different radial locations to measure transient changes in soil temperature.

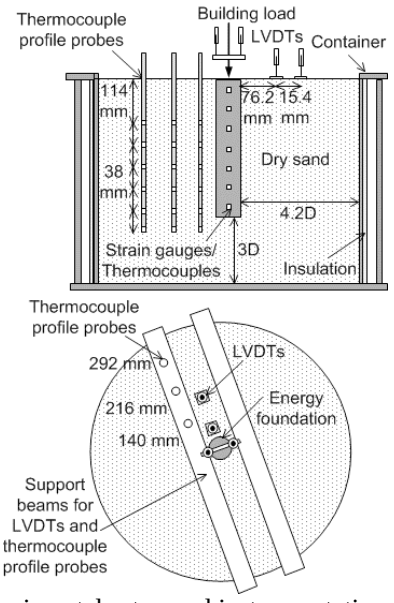

Figure 3. Experimental setup and instrumentation plan.

4.2 *Temperature Control System*

A Julabo F25-ME heat pump in series with a centrifugal pump was used to control the temperature of the heat exchanger fluid (silicon fluid) in the energy foundations. Silicon fluid maintains a viscosity close to that of water for different temperatures, and is compatible with the slip-ring stack between the stationary and spinning environments. Two servovalves were used to control the amount of pre-heated fluid circulated through the foundation. The bypass valve was used to recirculate heated fluid back into the heat pump, while the inlet valve was used to meter the fluid flow through the foundation to reach a target temperature. Pipe-plug thermocouples were used to monitor the fluid temperatures going in and out of the foundation. More details of the temperature control system are presented in Stewart (2012).

5 PROCEDURES

The results from four tests performed with the same foundation are compared in this study. They involved application of a seating load to the foundation followed by a heating test to reach changes in

temperature of 0 (ambient), 7, 12, and 18 °C. After the foundations stabilized under the elevated temperatures, they were loaded to failure, as shown in the time series of axial load applied to the foundations in Figure 4. The tests were designed to provide information on the thermo-mechanical stress-strain response during heating and permit evaluation of the impact of heating on the axial capacity.

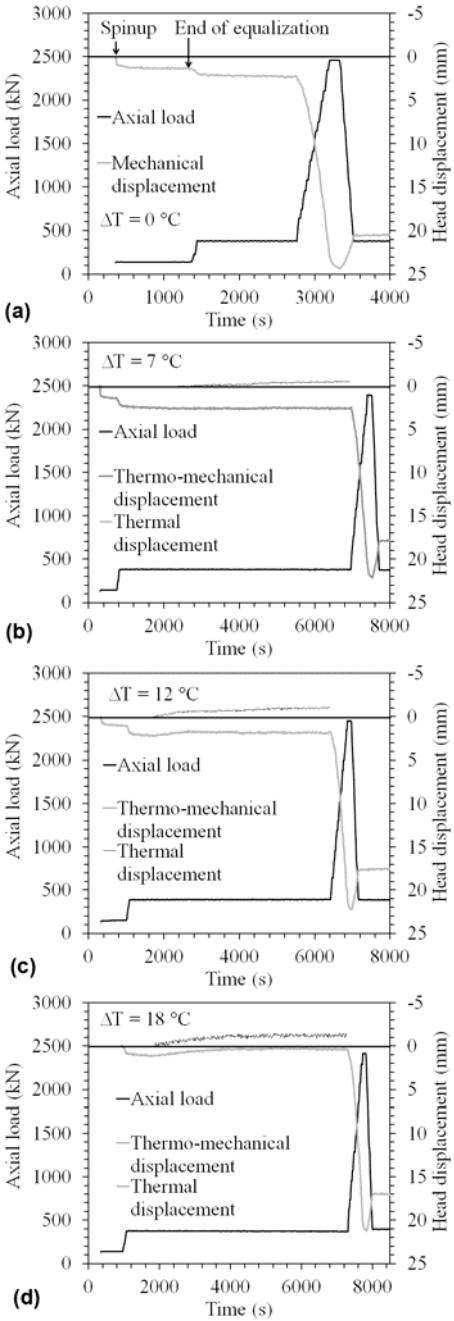

Figure 4. Loads and displacements (prototype scale): (a) ΔT = 0 °C; (b) ΔT = 7 °C; (c) ΔT = 12 °C; (d) ΔT = 18 °C.

6 RESULTS

Time series of the measured thermo-mechanical and thermal head displacements for the energy foundations (prototype scale) are also shown in Figure 4. The settlement of the foundation during spin-up of the centrifuge is not shown, and the LVDT measurements were corrected for the slight changes in the ambient temperature of the centrifuge chamber throughout the tests (change in 1°C on average). The foundations settled by about 1-2 mm in prototype scale during application of the seating load, then expanded upward during heating to the temperatures shown in Figure 5.

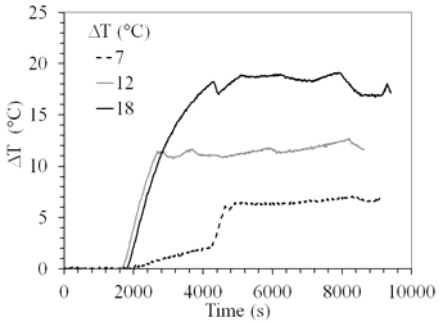

Figure 5. Foundation temperature time histories.

The thermo-mechanical strains measured by the functional gages are shown in Figure 6. Application of the seating load led to negligible strains in the foundation, with some inconsistent trends (i.e., larger strains near the toe). During heating, the negative strains indicate expansion, while during final loading to failure led to compressive strains in the foundation reversing the trend in strain. Greater strains are observed during heating to higher temperatures.

7 ANALYSIS

The thermal strain profiles defined by zeroing the strains at the beginning of heating are shown in Figure 7(a). The strains were relatively constant with height in the foundations, and were close to free expansion conditions (noted by the strain value at a depth of zero). The thermal axial stresses in the foundation were smallest at the top, and the average values shown in Figure 7(a) indicate that they increase slightly with temperature. The thermal displacements obtained by subtracting the integrated strains from the head displacement measured using the LVDT are shown in Figure 7(b). The null point is slightly below the center of the foundation, as expected. The change in temperature did not lead to a major change in the location of the null point. The load-settlement curves for the three thermo-mechanical and reference test are shown in Figure 7(c). Different from the observations of McCartney and Rosenberg (2011), no change in ultimate capacity is observed with temperature. This may be due to the difference in constraint provided by the sand to radial expansion of the foundation compared to the compacted silt tested by McCartney and Rosenberg (2011), which had a greater initial contact. There may also be a difference in side shear mobilization of the sand (likely linearly increasing with depth) compared to the silt (likely constant with depth).

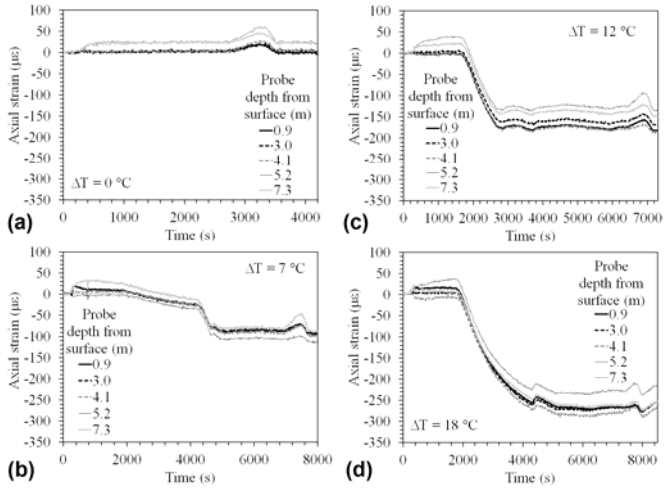

Figure 6. Thermo-mechanical strain results: (a) ΔT = 0 °C test; (b) ΔT = 7 °C test; (c) ΔT = 12 °C test; (d) ΔT = 18 °C test.

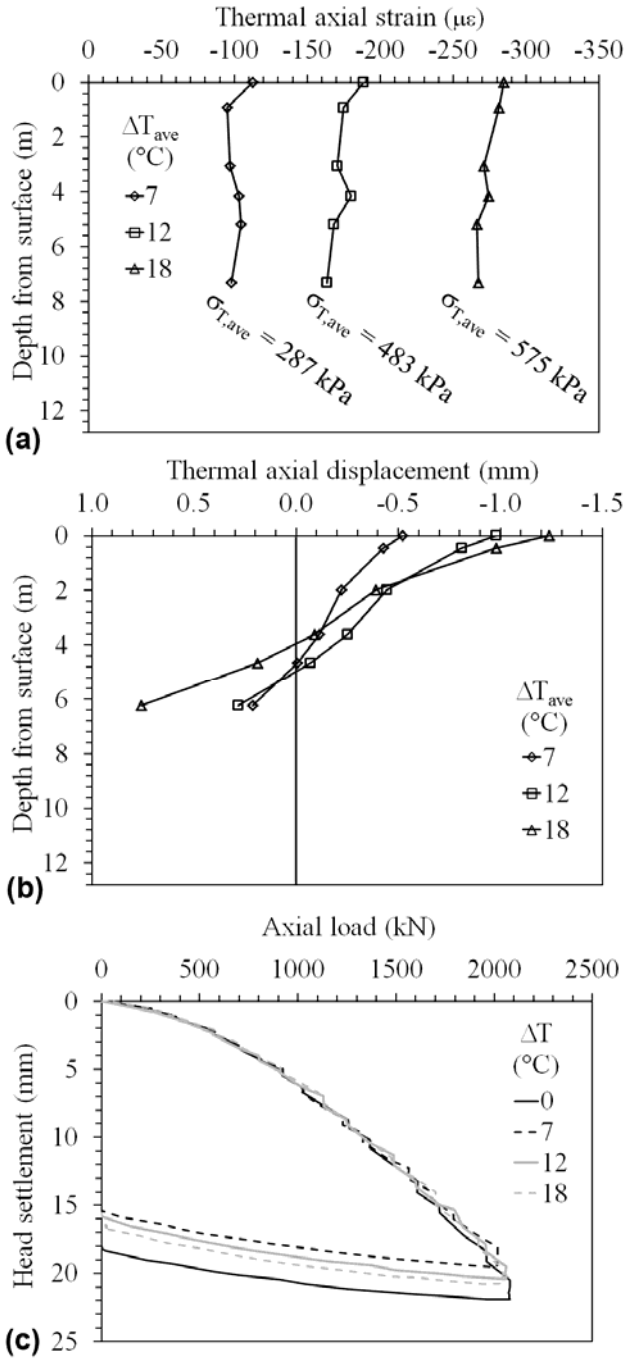

Figure 7. Synthesis of results: (a) Thermal strains; (b) Thermal axial displacements; (c) Load-settlement curves

8 CONCLUSIONS

The results in this study indicate that centrifuge modeling can be used to define useful parameters for thermo-mechanical soil-structure interaction analyses. During heating of semi-floating foundations in sand, an increase in expansive strains was noted, along with an increase in compressive stress due to restraint from side shear resistance. The foundation ultimate capacity was not sensitive to temperature.

9 ACKNOWLEDGEMENTS

Financial support for this work from NSF grant CMMI 0928159 is greatly appreciated.

10 REFERENCES

Amatya, B.L., Soga, K., Bourne-Webb, P.J., Amis, T., & Laloui, L. 2012. Thermo-mechanical behaviour of energy piles. *Géotechnique*. 62(6): 503–519.

Bourne-Webb, P., Amatya, B., Soga, K., Amis, T., Davidson, C., & Payne, P. 2009. Energy pile test at Lambeth College, London: Geotechnical and thermodynamic aspects of pile response to heat cycles. *Géotechnique*. 59(3): 237-248.

Brandl, H. 1998. Energy piles and diaphragm walls for heat transfer from and into the ground. *BAP III*, Ghent, Belgium. October 19-21. Balkema, Rotterdam. 37–60.

Brandl, H. 2006. Energy foundations and other thermo-active ground structures. *Géotechnique*. 56(2): 81-122.

Ennigkeit, A. & Katzenbach, R. 2001. The double use of piles as foundation and heat exchanging elements. *Proc. 15th ICSMGE*. Istanbul, Turkey. 893-896.

Knellwolf, C., Peron, H., & Laloui, L. 2011. Geotechnical analysis of heat exchanger piles. *JGGE*. 137(12): 890-902.

Ko, H.-Y. 1988. Summary of the state-of-the-art in centrifuge model testing. *Centrifuges in Soil Mechanics*. Craig, James, Scofield, eds. Balkema, pp. 11-28.

Krishnaiah, S. & Singh, D.N. 2004. Centrifuge modelling of heat migration in soils, *Int. J. of Physical Modelling in Geotechnics*. 4(3): 39-47.

Laloui, L., Nuth, M., & Vulliet, L. 2006. Experimental and numerical investigations of the behaviour of a heat exchanger pile. *IJNAMG*. 30(8): 763–781.

McCartney, J.S. & Rosenberg, J.E. 2011. "Impact of heat exchange on side shear in thermo-active foundations. *GeoFrontiers 2011*. March 13-16th, 2011. ASCE. 10 pg.

McCartney, J.S. & Murphy, K.D. 2012. Strain Distributions in Full-Scale Energy Foundations. *DFI Journal*. 6(2): 28-36.

Plaseied, N. 2011. *Load-Transfer Analysis of Energy Foundations*. M.S. Thesis. Univ. of Colorado Boulder. 90 pg.

Savvidou, C. 1988. Centrifuge modelling of heat transfer in soil. *Centrifuge 8*8, Corté, ed., Balkema. 583-591.

Stewart, M. 2012. *Centrifuge Modeling of Strain Distributions in Energy Foundations*. MS Thesis. CU Boulder. 110 pg.

Taylor R. 1995. *Geotechnical Centrifuge Technology*. Blackie, London. 296 p.